

Precision Metrology via Driving through Quantum Phase Transitions

Jiahao Huang¹, Min Zhuang^{1,2}, and Chaohong Lee^{1,2,3*}

¹*Laboratory of Quantum Engineering and Quantum Metrology, School of Physics and Astronomy, Sun Yat-Sen University (Zhuhai Campus), Zhuhai 519082, China*

²*State Key Laboratory of Optoelectronic Materials and Technologies, Sun Yat-Sen University (Guangzhou Campus), Guangzhou 510275, China and*

³*Synergetic Innovation Center for Quantum Effects and Applications, Hunan Normal University, Changsha 410081, China*

(Dated: December 14, 2024)

We propose a scheme to realize high-precision many-body quantum interferometry by driving the system through quantum phase transitions. The beam splitting, in which an initial non-degenerate groundstate evolves into a highly entangled state, is achieved by adiabatically driving the system from a non-degenerate regime to a degenerate one. Inversely, the beam recombination, in which the output state after interrogation becomes gradually disentangled, is accomplished by adiabatically driving the system from the degenerate regime to the non-degenerate one. The phase shift, which is accumulated in the interrogation process, can then be easily inferred via population measurement. We apply our scheme to two-mode Bose condensed atoms and spin-1 Bose-Einstein condensates, and find that Heisenberg-limited precision scalings can be approached. Our proposed scheme does not require single-particle resolved detection and is within the reach of current experiment techniques.

Recent breakthroughs in generating many-body quantum entangled states boost tremendous advances in quantum metrology [1–5]. The desired entangled states of massive particles are often created via dynamical evolution with nonlinear interactions, such as spin-twisting [6–10] and spin-mixing [11–13] in ultracold atomic gases. However, the dynamically generated states are always not steady states and the system parameters must be precisely controlled. An alternatively deterministic and more robust way for preparing entangled states is to drive the system through quantum phase transitions (QPTs) [14–17]. More recently, this transitional approach has been experimentally demonstrated via a spin-1 atomic Bose-Einstein condensate (BEC), where a high-fidelity twin Fock state has been created [17].

To fully exploit quantum resources for achieving precision beyond standard quantum limit, detectors of single-particle resolution are always needed for directly reading out entangled sensor states [18, 19]. Therefore it is important to consider whether one can replace single-particle resolved detection with low-resolution detection (such as population detection). With the input entangled states generated by nonlinear dynamical evolution, the echo protocols with time-reversal nonlinear dynamics have been theoretically proposed [20–23] and experimentally demonstrated [24, 25]. While the driving through QPTs has been proposed for deterministic entanglement generation [14–17], to fully utilize entanglement for quantum sensing without single-particle resolved detection, can one use the reversely driving through QPTs for beam recombination?

In the Letter, based upon a many-body quantum interferometer, we propose how to implement Heisenberg-limited quantum phase estimation via driving through QPTs. In our proposal, the beam splitting and recombination are achieved by adiabatically sweeping the sys-

tem parameter forwardly and inversely through QPTs, respectively. For several interacting many-body quantum systems, sweeping a typical system parameter from a non-degenerate regime to a degenerate regime, the final states always appear as entangled states. In the phase accumulation process, the state acquires a phase to be measured. To read out the phase, the beam recombination, a reversed sweeping from the degenerate regime to the non-degenerate regime, is introduced to disentangle the sensor state. To show the validity of our scheme, as two examples, we apply it to a two-mode atomic BEC and a spin-1 atomic BEC, and find that the estimated phase precisions indeed approach the Heisenberg limit. Since the final states before measurement can be resolved with coarsened detectors, our scheme relaxes the single-particle resolution typically requested in previous schemes via parity measurement [26–30]. Unlike the recent nonlinear read-out schemes [20–25] in which the whole Hamiltonian of beam recombination is time-reversal with respect to the one of beam splitting (where the sign of nonlinearity for recombination should be opposite), our proposal only requires that the sweeping of time-dependent parameter for beam recombination is reversed to the one in beam splitting (the sign of nonlinearity remains the same for both beam splitting and recombination).

We show our phase estimation protocol in Fig. 1. We assume all time-evolution dynamics are unitary and set the reduced Planck constant $\hbar = 1$. First, an initial state $|\psi_I\rangle$ is prepared as the groundstate $|\psi\rangle_I$ of $\lambda_0 H_1$. Then, an entangled state $|\psi_E\rangle$ is gradually created in the beam splitting process $H_{BS1}(t)$ via driving through QPTs. In the interrogation process, the state acquires a phase ϕ via a phase-imprinting evolution $\hat{U}(\phi)$, that is, $|\psi(\phi)\rangle = \hat{U}(\phi)|\psi_E\rangle$. To extract the accumulated phase ϕ , the beam recombination $H_{BS2}(t)$ and a subsequent measurement of the observable \hat{O} are implemented. Here the

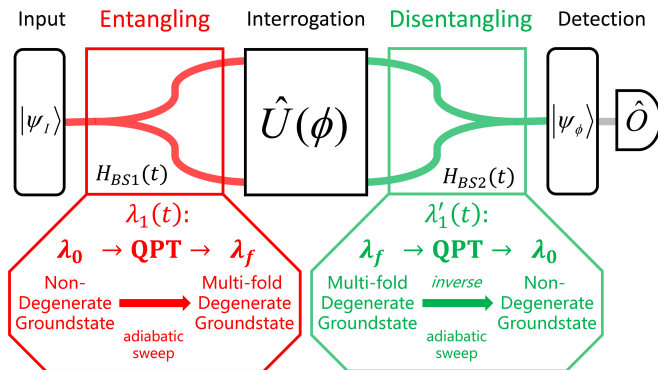


FIG. 1: (color online). Schematic diagram of quantum phase estimation via driving through quantum phase transitions (QPTs). The two beam splitters are achieved by driving the parameter $\lambda_1(t)$ across the critical point λ_c . In the first beam splitter, $H_{BS1}(t) = \lambda_1(t)H_1 + \lambda_2H_2$, the parameter $\lambda_1(t)$ adiabatically sweeps from λ_0 to λ_f and the state evolves from a non-degenerate groundstate (λ_0H_1 dominates) to a degenerate groundstate (λ_2H_2 dominates). Then the state accumulates the phase ϕ in the interrogation process. While in the second beam splitter, $H_{BS2}(t) = \lambda'_1(t)H_1 + \lambda_2H_2$, the parameter $\lambda'_1(t)$ inversely sweeps from λ_f (λ_2H_2 dominates) to λ_0 (λ_0H_1 dominates) and the state is gradually disentangled.

beam recombination $H_{BS2}(t)$ is achieved by the reversed sweeping of the beam splitting $H_{BS1}(t)$.

Beam Splitting and Recombination via driving through QPTs.— The beam splitting for generating entangled states can be described by a time-dependent Hamiltonian,

$$\begin{aligned} H_{BS1}(t) &= \lambda_1(t)H_1 + \lambda_2H_2, \\ &= (\lambda_0 - \alpha t)H_1 + \lambda_2H_2. \end{aligned} \quad (1)$$

Here, $\lambda_0 \gg |\lambda_2|$, and the time-varying parameter $\lambda_1(t)$ interpolates the Hamiltonians H_1 and H_2 when $\lambda_1(t)$ is adiabatically swept from λ_0 to 0. We choose proper Hamiltonians such that the groundstate of λ_0H_1 is non-degenerate while the groundstate of λ_2H_2 is multi-fold degenerate. There exists a QPT at the critical point λ_c , that is, $\lambda_1(t)H_1$ dominates the system when $\lambda_1(t) > \lambda_c$ and λ_2H_2 dominates the system when $0 \leq \lambda_1(t) < \lambda_c$. Starting from the non-degenerate groundstate of λ_0H_1 , an entangled groundstate (which is a specific superposition of the degenerate groundstates of λ_2H_2) can be obtained with high fidelity if $\lambda_1(t)$ is adiabatically swept from λ_0 to λ_f ($0 \leq \lambda_f < \lambda_c$).

While the adiabatic operation of $H_{BS1}(t)$ serves as the first beam splitter and generates the entangled input state $|\psi\rangle_E$, an inverse operation of $H_{BS1}(t)$ onto $|\psi\rangle_E$ would in principle disentangle it back to the initial state $|\psi\rangle_I$, which can act as the second beam splitter for recombination. The second beam splitter can be described

by a time-dependent Hamiltonian,

$$\begin{aligned} H_{BS2}(t) &= \lambda'_1(t)H_1 + \lambda_2H_2, \\ &= (\lambda_f + \alpha t)H_1 + \lambda_2H_2, \end{aligned} \quad (2)$$

where $\lambda'_1(t)$ is inversely swept from λ_f towards λ_0 with opposite sweeping rate for $H_{BS1}(t)$.

Thus, the state before detection is expressed as $|\psi(\phi)\rangle_R = e^{-i\int_0^{\tau_2} H_{BS2}(t)dt} \hat{U}(\phi) e^{-i\int_0^{\tau_1} H_{BS1}(t)dt} |\psi_I\rangle$ with the splitting duration τ_1 and the recombination duration τ_2 . Ideally for $\phi = 0$, the state $|\psi(\phi)\rangle_R$ is identical to the initial state $|\psi_I\rangle$ (there may exist a globally relative phase) if $\lambda'_1(\tau_2) = \lambda_0$. When $\phi \neq 0$, the nonzero phase will bias the state $|\psi(\phi)\rangle_R$ with respect to the initial state $|\psi_I\rangle$, and one can detect a ϕ -dependent observable $\langle \hat{O} \rangle$ to extract the phase information. In practice, the recombination duration can be shorter than the splitting duration, i.e., $\tau_2 \leq \tau_1$. Thus in the inverse sweeping, it is not required to reach λ_0 exactly and there may exist several optimal values $\lambda'_1(\tau_2) = \lambda'_{opt}$ that can achieve the best measurement precision. Obviously, the recombination via inverse sweeping adds no additional complexity of experimental manipulation.

Two-mode Bose condensed atoms.— We now illustrate our phase estimation protocol via two-mode Bose condensed atoms. The system obeys a symmetric Bose-Josephson Hamiltonian [7–9, 14, 31, 32]

$$H_{BJ} = -\Omega \hat{J}_x + \frac{\chi}{N} \hat{J}_z^2, \quad (3)$$

with the Josephson coupling strength Ω , the nonlinear atom-atom interaction χ , and the collective spin operators: $\hat{J}_x = \frac{1}{2}(\hat{a}\hat{b}^\dagger + \hat{a}^\dagger\hat{b})$, $\hat{J}_y = \frac{1}{2i}(\hat{a}\hat{b}^\dagger - \hat{a}^\dagger\hat{b})$, $\hat{J}_z = \frac{1}{2}(\hat{b}^\dagger\hat{b} - \hat{a}^\dagger\hat{a})$. Here \hat{a} and \hat{b} are annihilation operators for particles in modes $|a\rangle$ and $|b\rangle$, respectively. Naturally, the system state can be expanded in the Dicke basis $|J, m\rangle$ with $J = N/2$ and $m = \{-J, -J+1, \dots, J\}$. There exists a transition between non-degenerate and degenerate groundstates when the nonlinearity is negative (i.e. $\chi < 0$) [14, 32]. For a N -atom system with $\chi < 0$, in strong coupling limit ($\Omega \gg |\chi|$), the groundstate is a SU(2) spin coherent state. When $\Omega \rightarrow 0$, the interaction dominates and the two lowest eigenstates become degenerate. The transition from non-degeneracy to degeneracy happens at the critical point $\Omega_c/|\chi| = 1$, which corresponds to a classical Hopf bifurcation from single-stability to bistability. Starting from the groundstate of H_{BJ} with large Ω and adiabatically decreasing Ω across the critical point $\Omega_c = |\chi|$, one can get a superposition of two self-trapping states, which can be approximately regarded as a spin cat state [29]. In our calculation, we set $\chi = -1$ and thus $\Omega_c = 1$.

To shorten the duration, we sweep the Josephson coupling strength Ω in two stages with different sweeping rates (it is also efficient that the sweeping rate becomes

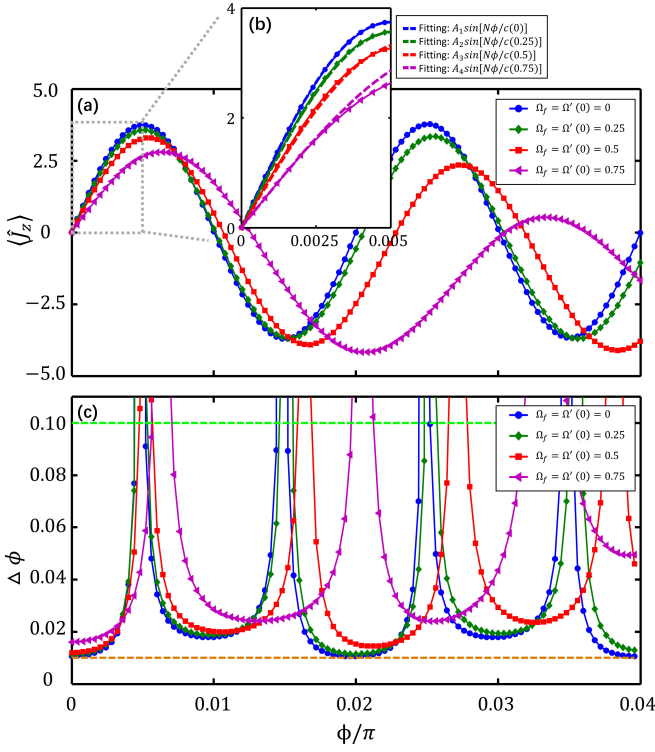


FIG. 2: (color online). Phase estimation via population measurement. (a) The final expectation of half population difference $\langle \hat{J}_z \rangle$ versus the accumulated phase ϕ in a Bose-Josephson system. (b) The inset shows the magnified region of $\langle \hat{J}_z \rangle$ near $\phi = 0$, in which the dashed lines are fitted according to the sine function. Four different input states $|\Psi(\Omega_f)\rangle_G$, which correspond to $\Omega_f = (0, 0.25, 0.5, 0.75)$, are denoted by circles (blue), diamonds (green), squares (red) and triangles (purple), respectively. In the recombination process, $\Omega'(t)$ is swept from Ω_f to the optimal value Ω'_{opt} . (c) The phase measurement precision $\Delta\phi$ versus ϕ derived from the error propagation formula $\Delta\phi = \frac{\sqrt{\langle \hat{J}_z^2 \rangle - \langle \hat{J}_z \rangle^2}}{|\partial \langle \hat{J}_z \rangle / \partial \phi|}$ versus ϕ . The green and orange dashed lines indicates the standard quantum limit and the Heisenberg limit, respectively.

time-dependent and is determined according to the energy spectra [33, 34]). When $\Omega(t) > 1$, the gap between the groundstate and the first excited state is large and so that the sweeping can be faster. While $\Omega(t) \leq 1$, the groundstate and first excited state become nearly degenerate and so that the sweeping should be much slower. Thus, the sweeping process can be described by

$$\Omega(t) = \begin{cases} \Omega_0 - \beta_1 t, & 0 \leq t \leq \tau_c, \\ \Omega_c - \beta_2(t - \tau_c), & \tau_c < t \leq \tau_1, \end{cases} \quad (4)$$

with the initial Josephson coupling strength Ω_0 , $\tau_c = (\Omega_0 - \Omega_c)/\beta_1$ and $\tau_1 = \tau_c + (\Omega_c - \Omega_f)/\beta_2$. Here, β_1 and β_2 denote the sweeping rates in the first stage from Ω_0 to Ω_c and the second stage from Ω_c to Ω_f ($0 \leq \Omega_f < \Omega_c$), respectively. The sweeping ends at different values of Ω_f would result in different ground states $|\Psi(\Omega_f)\rangle_G$. We

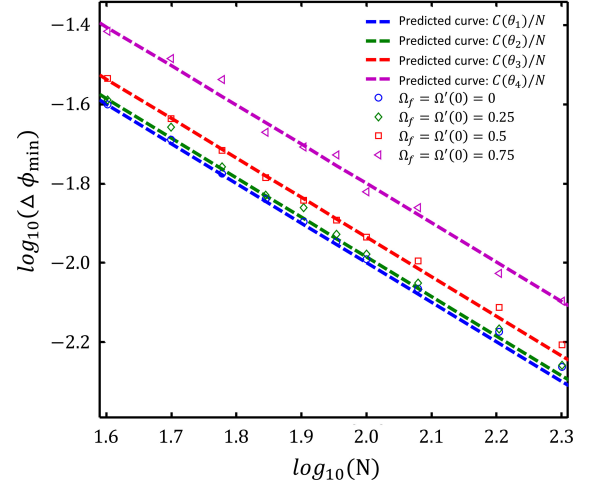


FIG. 3: (color online). The log-log precision scaling $\Delta\phi_{min}$ versus total atomic number N for Bose-Josephson system via driving through QPTs with different input states $|\Psi(\Omega_f)\rangle_G$. The blue circles, green diamonds, red squares and purple triangles correspond to $\Omega_f = (0, 0.25, 0.5, 0.75)$, respectively. Their precisions follow the Heisenberg-limited scaling. The dashed lines are the predicted precision scaling obtained by approximating the input states $|\Psi(\Omega_f)\rangle_G$ as corresponding spin cat states (see Supplementary Material).

prepare four different input states $|\Psi(\Omega_f)\rangle_G$ for $\Omega_f = (0, 0.25, 0.5, 0.75)$ and then analyze their interferometric performances.

Through the interrogation process, the input state $|\Psi(\Omega_f)\rangle_G$ evolves into,

$$|\Psi(\phi)\rangle = \hat{U}(\phi)|\Psi(\Omega_f)\rangle_G = e^{-i\phi\hat{J}_z}|\Psi(\Omega_f)\rangle_G, \quad (5)$$

with the accumulated phase $\phi = \omega T$. Here ω is the energy difference between $|a\rangle$ and $|b\rangle$ and T denotes the interrogation time. Then, after the interrogation process, the system undergoes another adiabatic process,

$$\Omega'(t) = \begin{cases} \Omega_f + \beta_2 t, & 0 \leq t \leq \tau'_c, \\ \Omega_c + \beta_1(t - \tau'_c), & \tau'_c < t \leq \tau_2, \end{cases} \quad (6)$$

which is the inverse process of the beam splitting (4). That is, the Josephson coupling strength is swept from $\Omega'(0) = \Omega_f$ to $\Omega'(\tau'_c) = \Omega_c$ with the sweeping rate β_2 , and then from Ω_c to $\Omega'(\tau_2) = \Omega'_{opt}$ with the sweeping rate β_1 . In practice, it is unnecessary sweeping back to Ω_0 , since there exist some specific values Ω'_{opt} ($\Omega_c < \Omega'_{opt} < \Omega_0$) that can achieve the optimal phase estimation (see Supplementary Material).

When the Josephson coupling strength $\Omega'(t)$ is swept to the optimal point Ω'_{opt} , we apply a $\frac{\pi}{2}$ -pulse and then measure the half population difference \hat{J}_z to estimate the accumulated phase ϕ . In Fig. 2 (a), we show the expectations $\langle \hat{J}_z \rangle$ with respect to the accumulated phase ϕ . In our calculation, we choose $N = 100$, $\Omega_0 = 11$,

$\beta_1 = 10$ and $\beta_2 = 0.5$. According to the error propagation formula, we obtain the measurement precision

$$\Delta\phi = \frac{\sqrt{\langle \hat{J}_z^2 \rangle - \langle \hat{J}_z \rangle^2}}{|\partial \langle \hat{J}_z \rangle / \partial \phi|} \text{ versus } \phi, \text{ see Fig. 2 (c).}$$

The population measurement is efficient to estimate the accumulated phase ϕ , especially in the vicinity of $\phi = 0$. For the input state $|\Psi(\Omega_f = 0)\rangle_G$, the dependence of $\langle \hat{J}_z \rangle$ on ϕ is exactly proportional to $\sin(N\phi)$. For $|\Psi(\Omega_f)\rangle_G$ with larger Ω_f , the dependence of $\langle \hat{J}_z \rangle$ on ϕ gradually deviate the standard sinusoidal oscillation when ϕ increases. The oscillation frequency decreases with Ω_f and the amplitude is no longer fixed when ϕ far apart from 0. Nevertheless, near $\phi = 0$, the expectation $\langle \hat{J}_z \rangle$ can still be approximated in sine function for most $|\Psi(\Omega_f)\rangle_G$, i.e., $\langle \hat{J}_z \rangle \simeq A(\Omega_f) \sin[N\phi/c(\Omega_f)]$, as shown in Fig. 2 (b). Here, for $N = 100$, $c(0) = 1$, $c(0.25) = 1.03$, $c(0.5) = 1.16$ and $c(0.75) = 1.58$, where the oscillation frequency $N/c(\Omega_f)$ decreases as Ω_f . The expectation $\langle \hat{J}_z^2 \rangle$ also oscillates with respect to ϕ and its minimum $B(\Omega_f)$ locates at $\phi = 0$ for all $|\Psi(\Omega_f)\rangle_G$. Thus, one can easily obtain the minimum phase uncertainty $\Delta\phi_{\min} = \frac{\sqrt{B(\Omega_f)c(\Omega_f)}}{A(\Omega_f)N}$ for $|\Psi(\Omega_f)\rangle_G$ at $\phi = 0$. The minimum phase uncertainty at $\phi = 0$ is inversely proportional to total atomic number N , which attains the Heisenberg limit.

To further confirm the Heisenberg-limited precision scaling, we obtain the minimum phase uncertainty $\Delta\phi_{\min}$ under different total particle number N , and plot the log-log scaling of $\Delta\phi_{\min}$ versus N , see Fig. 3. For the input states $|\Psi(\Omega_f)\rangle_G$ with $\Omega_f = (0, 0.25, 0.5, 0.75)$, all their precisions follow the Heisenberg scaling but multiplied by different coefficients dependent on Ω_f , i.e., $\Delta\phi_{\min} \propto \tilde{C}(\Omega_f)/N$ (see more details in Supplementary Material). Although the precision gets a bit worse with larger Ω_f , it requires much shorter state preparation and recombination time, which may be more experimentally feasible.

Spin-1 Bose-Einstein condensates.— The scheme for beam splitting via adiabatic transitions can also be realized with spinor BECs. As the second example, we consider a spin-1 BEC under an external magnetic field, which had been realized with ^{87}Rb (or ^{23}Na) atoms in an optical trap [35]. In an $F = 1$ ^{87}Rb condensate, we choose an initial state with all atoms prepared in $m_F = 0$ component. Thus, the system state would be constrained by the zero magnetization. Then, the system can be described by the Hamiltonian [15, 17],

$$H_S = -q\hat{N}_0 + \frac{c_2}{2N}[(2\hat{a}_0^\dagger\hat{a}_0^\dagger\hat{a}_1\hat{a}_{-1} + h.c.) + (2\hat{N}_0 - 1)(N - \hat{N}_0)] \quad (7)$$

with $\hat{N}_0 = \hat{a}_0^\dagger\hat{a}_0$, the total atomic number N being an even integer and \hat{a}_{m_F} denoting annihilation operator for spin- m_F component. Here, c_2 is the spin-dependent collision energy, and $p(q)$ are respectively the linear

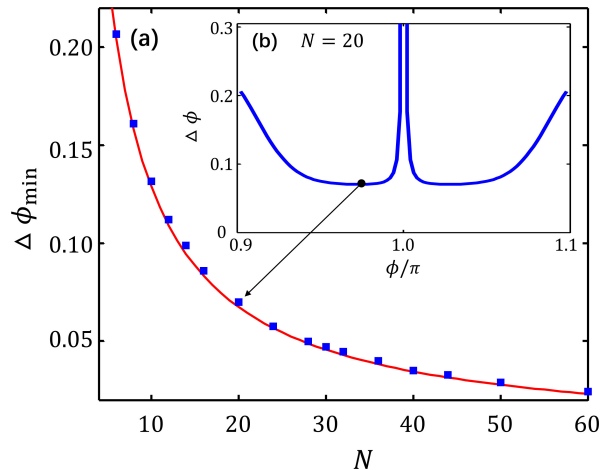


FIG. 4: (color online). (a) The dependence of phase precision $\Delta\phi_{\min}$ on the total atomic number N for spin-1 BEC via driving through QPTs. The blue squares are the numerical results with sweeping rate $\alpha = 0.01$. The red solid line denotes the ultimate precision bound of twin Fock state, i.e., $\Delta\phi_{\text{QCRB}} = (N^2/2 + N)^{-1/2}$. (b) The numerical result of phase precision $\Delta\phi$ versus ϕ for $N = 20$. The black dot corresponds to the minimum phase precision $\Delta\phi_{\min}$ near $\phi = \pi$.

(quadratic) Zeeman energy shifts. The second term describes spin-exchange collisions, where correlated pairs in $m_F = \pm 1$ are created from atoms in $m_F = 0$ and vice versa. For an ferromagnetic condensate (setting $c_2 = -1$), there are three distinct phases with two critical points of QPTs: $q = \pm 2$. For $q > 2$, the groundstate is a polar phase. Between the two critical points, $-2 \leq q \leq 2$, the groundstate is a broken-antisymmetry phase. While for $q < -2$, the groundstate is a twin Fock state with all atoms equally populated into the $m_F = \pm 1$ spin components. By tuning external magnetic field, the quadratic Zeeman energy shift can be linearly swept, i.e.,

$$q(t) = q_0 - \alpha t, \quad (8)$$

where $q_0 > 2$ is the initial quadratic Zeeman shift and α is the sweeping rate. By adiabatically sweeping the quadratic Zeeman shift $q(t)$ from q_0 to $-q_0$, the system goes through the two critical points and its initial state will gradually evolve into a twin Fock state, which had been realized in a recent experiment [17].

Given the twin Fock state $|\Psi\rangle_{\text{TF}} = |\frac{N}{2}\rangle_{-1}|\frac{N}{2}\rangle_1$, one can implement a phase accumulation process $\hat{U}(\phi)$ and the phase accumulated state reads,

$$|\Psi(\phi)\rangle = \hat{U}(\phi)|\Psi\rangle_{\text{TF}} = \hat{R}_{\pi/2}^\dagger e^{-i\frac{\phi}{2}(\hat{a}_1^\dagger\hat{a}_1 - \hat{a}_{-1}^\dagger\hat{a}_{-1})} \hat{R}_{\pi/2} |\Psi\rangle_{\text{TF}}, \quad (9)$$

with $\hat{R}_{\pi/2} = e^{i\frac{\pi}{4}(\hat{a}_1^\dagger\hat{a}_{-1} - \hat{a}_{-1}^\dagger\hat{a}_1)}$ being a $\pi/2$ rotation. Then the inverse adiabatic driving is applied on the ϕ -dependent state $|\Psi(\phi)\rangle$ for recombination. The inverse operation can be achieved by sweeping q from $-q_0$ to q_0

with same sweeping rate α ,

$$q'(t) = -q_0 + \alpha t. \quad (10)$$

After the adiabatic recombination, the phase ϕ can be estimated by measuring the final population \hat{N}_0 in component $m_F = 0$. Ideally, if $\phi = k\pi$ ($k = 0, 1, 2, \dots$), all the atoms would populate into $m_F = 0$ again, leading to $\langle \hat{N}_0 \rangle = N$. For other values of ϕ , the population $\langle \hat{N}_0 \rangle$ would be less than N and dependent on ϕ , see Supplementary Material.

In our calculation, we choose $q_0 = 3$ and $\alpha = 0.01$. We calculate the phase precision $\Delta\phi = \frac{\Delta\hat{N}_0}{|\partial\langle\hat{N}_0\rangle/\partial\phi|}$ with respect to ϕ in the vicinity of $\phi = \pi$ for $N = 20$, see Fig. 4 (b). The minimum phase uncertainty $\Delta\phi_{\min}$ occurs near $\phi = \pi$. However, $\Delta\phi$ blows up at $\phi = \pi$ since $\Delta\hat{N}_0$ vanishes. Further, we give the minimum phase uncertainty $\Delta\phi_{\min}$ under different total particle number N , and show how the phase precision depends on N , see Fig. 4 (a). It is shown that, the phase precision follows the corresponding ultimate bound [36, 37], which indicates that the combination of reversed adiabatic driving and population measurement is an optimal detection for twin Fock state. When N is large, $\Delta\phi_{\min} \sim \sqrt{2}/N$, which approaches the Heisenberg limit.

Conclusion.— We have presented a scheme for precision metrology via driving through QPTs. For both two-mode and spin-1 Bose condensed atoms, the adiabatic processes are robust against excitation since it is protected by the symmetry of the involved eigenstates across the QPTs [16, 17]. Thus, the sweeping rates in state preparation and recombination can be relatively fast and the duration can be within the reach of current experiments. The recombination via reversed sweeping through QPTs does not bring any additional complexity for the apparatus design, which may be also realized in laboratory. In addition, our scheme is robust against imperfect detection, where the high-precision measurement beyond standard quantum limit can be achieved without single-particle resolved detection. Our proposal points out a new way of utilizing highly entangled states for quantum metrology, in which the efficient readout is achieved by the combination of driving through QPTs and population measurement.

This work is supported by the National Natural Science Foundation of China (NNSFC) under Grants No. 11374375 and No. 11574405. J. H. is partially supported by National Postdoctoral Program for Innovative Talents of China (BX201600198).

* Email: lichaoh2@mail.sysu.edu.cn, chleecn@gmail.com

[1] V. Giovannetti, S. Lloyd, and L. Maccone, *Science* **306**, 1330 (2004).

- [2] V. Giovannetti, S. Lloyd, and L. Maccone, *Phys. Rev. Lett.* **96**, 010401 (2006).
- [3] V. Giovannetti, S. Lloyd, and L. Maccone, *Nature Photo.* **5**, 222 (2011).
- [4] A. D. Ludlow, M. M. Boyd, J. Ye, E. Peik, and P. O. Schmidt, *Rev. Mod. Phys.* **87**, 637 (2015).
- [5] L. Pezzé, A. Smerzi, M. K. Oberthaler, R. Schmied, and P. Treutlein, arXiv:1609.01609.
- [6] M. Kitagawa, and M. Ueda, *Phys. Rev. A* **47**, 5138 (1993).
- [7] C. Gross, T. Zibold, E. Nicklas, J. Estève, and M. K. Oberthaler, *Nature (London)* **464**, 1165(2010).
- [8] M. F. Riedel, P. Böhi, Y. Li, T. W. Hänsch, A. Sinatra, and P. Treutlein, *Nature (London)* **464**, 1170 (2010).
- [9] H. Strobel, W. Muessel, D. Linnemann, T. Zibold, D. B. Hume, L. Pezzé, A. Smerzi, and M. K. Oberthaler, *Science* **345**, 424 (2014).
- [10] W. Muessel, H. Strobel, D. Linnemann, T. Zibold, B. Juliá-Díaz, and M. K. Oberthaler, *Phys. Rev. A* **92**, 023603 (2015).
- [11] B. Lücke, M. Scherer, J. Kruse, L. Pezzé, F. Deuretzbacher, P. Hyllus, O. Topic, J. Peise, W. Ertmer, J. Arlt, L. Santos, A. Smerzi, C. Klempt, *Science* **334**, 773 (2011).
- [12] E. M. Bookjans, C. D. Hamley, and M. S. Chapman, *Phys. Rev. Lett.* **107**, 210406 (2011).
- [13] M. Gabbriellini, L. Pezzé, and A. Smerzi, *Phys. Rev. Lett.* **115**, 163002 (2015).
- [14] C. Lee. *Phys. Rev. Lett.* **97**, 150402 (2006).
- [15] Z. Zhang, and L. -M. Duan, *Phys. Rev. Lett.* **111**, 180401 (2013).
- [16] H. Xing, A. Wang, Q. Tan, W. Zhang, and S. Yi, *Phys. Rev. A* **93**, 043615 (2016).
- [17] X. Luo, Y. Zou, L. Wu, Q. Liu, M. Han, M. Tey, and L. You, *Science* **355**, 620 (2017).
- [18] H. Zhang, R. McConnell, S. Čuk, Q. Lin, M. H. Schleier-Smith, I. D. Leroux, and V. Vuletić, *Phys. Rev. Lett.* **109**, 133603 (2012).
- [19] D. B. Hume, I. Stroescu, M. Joos, W. Muessel, H. Strobel, and M. K. Oberthaler, *Phys. Rev. Lett.* **111**, 253001 (2013).
- [20] F. Fröwis, P. Sekatski, and W. Dür, *Phys. Rev. Lett.* **116**, 090801 (2016).
- [21] E. Davis, G. Bentsen, and M. Schleier-Smith, *Phys. Rev. Lett.* **116**, 053601 (2016).
- [22] S. S. Szigeti, R. J. Lewis-Swan, and S. A. Haine, *Phys. Rev. Lett.* **118**, 150401 (2017).
- [23] S. P. Nolan, S. S. Szigeti, and S. A. Haine, arXiv: 1703.10417.
- [24] D. Linnemann, H. Strobel, W. Muessel, J. Schulz, R. J. Lewis-Swan, K. V. Kheruntsyan, and M. K. Oberthaler, *Phys. Rev. Lett.* **117**, 013001 (2016).
- [25] O. Hosten, R. Krishnakumar, N. J. Engelsens, and M. A. Kasevich, *Science* **352**, 1552 (2016).
- [26] R. A. Campos, C. C. Gerry, and A. Benmoussa, *Phys. Rev. A* **68**, 023810 (2003).
- [27] P. M. Anisimov, G. M. Raterman, A. Chiruvelli, W. N. Plick, S. D. Huver, H. Lee, and J. P. Dowling, *Phys. Rev. Lett.* **104**, 103602 (2010).
- [28] C. C. Gerry and J. Mimih, *Phys. Rev. A* **82**, 013831 (2010).
- [29] J. Huang, X. Qin, H. Zhong, Y. Ke, and C. Lee, *Sci. Rep.* **5**, 17894 (2015).

- [30] C. Luo, J. Huang, X. Zhang, and C. Lee, Phys. Rev. A **95**, 023608 (2017).
- [31] C. Lee, L.-B. Fu, and Y. S. Kivshar, EPL **81**, 60006 (2008).
- [32] C. Lee, Phys. Rev. Lett. **102**, 070401 (2009).
- [33] X. Peng, Z. Luo, W. Zheng, S. Kou, D. Suter, and J. Du, Phys. Rev. Lett. **113**, 080404 (2014).
- [34] Z. Luo, J. Li, Z. Li, L. Hung, Y. Wan, X. Peng, and J. Du, arXiv: 1608.06963.
- [35] D. M. Stamper-Kurn, and M. Ueda, Rev. Mod. Phys. **85**, 1191 (2013).
- [36] L. Pezzé, and A. Smerzi, Phys. Rev. Lett. **102**, 100401 (2009).
- [37] J. Huang, S. Wu, H. Zhong, and C. Lee, Quantum Metrology with Cold Atoms, Annual Review of Cold Atoms and Molecules **2**, 365-415 (2014).